

# The Effect of the Substrate on Response of Thioaromatic Self-Assembled Monolayers to Free Radical-Dominant Plasma

Ming-Chen Wang,<sup>‡</sup> Jiunn-Der Liao,<sup>\*,†</sup> Chih-Chiang Weng,<sup>‡</sup> Ruth Klauser,<sup>§</sup> Stefan Frey,<sup>||</sup> Michael Zharnikov,<sup>\*,||</sup> and Michael Grunze<sup>||</sup>

Department of Biomedical Engineering, Chung Yuan Christian University, 22, Pu-Jen, Pu-Chung-Li, Chung-Li, Taoyuan 32023, Taiwan (ROC), Department of Materials Science and Engineering, National Cheng Kung University, No. 1, University Road, Tainan 701, Taiwan (ROC), Synchrotron Radiation Research Center, No. 1 R&D Road VI, Hsinchu Science-Based Industrial Park, Hsinchu 300, Taiwan (ROC), and Angewandte Physikalische Chemie, Universität Heidelberg, Im Neuenheimer Feld 253, 69120 Heidelberg, Germany

Received: November 13, 2001; In Final Form: March 29, 2002

Synchrotron-based high-resolution photoelectron spectroscopy was applied to study the modification of self-assembled monolayers (SAMs) of 4'-methyl-1,1'-biphenyl-4-thiols (BPT) on (111) gold and silver substrates by a nitrogen–oxygen downstream microwave plasma and the attachment of acrylic acid to the plasma-modified SAMs. The plasma treatment resulted in massive damage and disordering of the BPT films, with the extent and character being noticeably different for BPT/Au and BPT/Ag. Whereas for BPT/Au a profound desorption of the entire BPT moieties and a complete defragmentation of the residual hydrocarbon part occurred, only partial desorption and oxidation took place for BPT/Ag, where even a part of intact BPT moieties survived the plasma treatment. The differences in the response of BPT/Au and BPT/Ag to the plasma treatment are related to the stronger thiolate–substrate bonds for the latter system. Taking into account that an analogous difference was also observed in alkanethiolate films, one can consider it as a general property of thiol-derived SAMs. The extent of acrylic acid attachment to the plasma-treated BPT/Ag was found to be essentially larger than that to the hydrocarbon residues in the case of BPT/Au.

## 1. Introduction

Control of wetting, lubrication, adhesion, and corrosion of surfaces and interfaces is a scientific and technological challenge. A practical way to achieve such a control is provided by so-called self-assembled monolayers (SAMs), which are close-packed arrays of long-chain, amphiphilic molecules attached to a substrate by a suitable headgroup.<sup>1,2</sup> By an appropriate choice of these molecules and, especially, by the selection of an appropriate terminal functional group, one can adjust the chemical reactivity, structural arrangement, molecular conformation, and the stability of the SAM surface. A further option is the physical modification of SAMs through their exposure to ions,<sup>3</sup> X-ray photons,<sup>4–7</sup> UV light,<sup>8–12</sup> electrons,<sup>13–23</sup> local oxidation,<sup>24</sup> or plasma treatment,<sup>25–27</sup> which enables us to use SAMs as a lithographic resist or a template to fabricate micro- and nanostructures.<sup>25,28–38</sup>

The character of the physical modification depends both on the applied method and the choice of the SAM. In particular, thiol-derived SAMs react very differently toward electron irradiation depending on the identity of the long-chain spacer: Whereas thioaliphatic SAMs become heavily damaged,<sup>19,22</sup> the irradiation-induced cross-linking between the neighboring aromatic moieties prevents both the damage of the S-substrate interface and the loss of the orientational order in pure thio-

aromatic films<sup>39,40</sup> and aromatic-substituted thioaliphatic SAMs.<sup>23</sup> The cross-linking follows C–H bond scissions in the aromatic rings and makes the film even more resistant toward external effects.<sup>23,39,40</sup> The remaining orientational order and the anchoring to the substrate enable an “exclusive” chemical modification of the tail group attached to the aromatic chain.<sup>38,40</sup>

Recently, we have applied nitrogen–oxygen downstream microwave plasma to modify thioaliphatic alkanethiolate (AT) SAMs on (111) Au and Ag substrates.<sup>27</sup> Our goals were to investigate changes occurring in the SAMs during the plasma treatment and test if such a treatment can be utilized as a “soft”, nondestructive SAM modification, i.e., an “exclusive” modification of the chemical identity of the tail group for potential microelectronic and biomedical applications. Although valuable information on the interaction of a low-energy plasma with SAMs was obtained, the plasma treatment resulted in massive damage and disordering of the initially well-ordered and chemically homogeneous AT films, which was predominantly caused by the oxygen-derived free radicals.<sup>27</sup>

Considering the above-mentioned differences between electron-beam modification of the thioaliphatic and thioaromatic SAMs and taking into account a lack of data on UV, ion, and plasma treatment of the latter systems, we applied the same nitrogen–oxygen downstream microwave plasma as in ref 27 to 4'-methyl-1,1'-biphenyl-4-thiolate (BPT:  $\text{CH}_3(\text{C}_6\text{H}_4)_2\text{S}-$ ) SAMs on (111) gold and silver substrates. The major goal was to explore possible differences in the reaction of thioaliphatic and thioaromatic SAMs toward a low-energy plasma. In addition, we wanted to investigate whether a “soft”, nondestructive SAM modification and subsequent selective molecular attachment are possible for the thioaromatic systems. For the latter purpose,

\* To whom correspondence should be addressed: M. Zharnikov (E-mail: Michael.Zharnikov@urz.uni-heidelberg.de) and J.-D. Liao (E-mail: jdliao@mail.ncku.edu.tw).

<sup>†</sup> National Cheng Kung University.

<sup>‡</sup> Chung Yuan Christian University.

<sup>§</sup> Synchrotron Radiation Research Center.

<sup>||</sup> Universität Heidelberg.

we exposed the plasma-processed BPT SAMs to acrylic acid (AAc:  $\text{C}_2\text{H}_3\text{COOH}$ ), which should provide carboxylic links for the attachment of biological molecules such as, e.g., collagens.

The extent and rate of plasma-induced processes for the BPT SAMs on Au in comparison to Ag are of fundamental interest. Whereas the physical modification of BPT/Ag has not been studied, the thioaliphatic films on Au and Ag substrates demonstrate a strong influence of the substrate on the resistance of these systems toward photooxidation,<sup>11,10</sup> ion and electron irradiation,<sup>3,22</sup> and plasma treatment.<sup>27</sup> The effect of the substrate was mainly explained by the stronger thiolate-substrate bond in AT/Ag as compared to AT/Au,<sup>3,22,27,41</sup> although a higher packing density and a smaller inclination of the alkyl chains in AT/Ag are probably also of importance (the average tilt angles of AT chains in AT/Ag and AT/Au are 10–12° and 27–33°, respectively).<sup>1,2,42</sup> In particular, the extent of the irradiation-induced changes in the biphenyl-substituted thioaliphatic SAMs clearly depends on the packing density and molecular orientation of the biphenyl moieties in these systems.<sup>23</sup> Note, however, that the difference between the tilt angles of the molecular spacer in BPT/Au and BPT/Ag is relatively small (~5°; the average tilt angles of the aromatic chains in BPT/Ag and BPT/Au are ~18° and ~23°, respectively),<sup>43</sup> which makes the density-related effects of a lesser importance than in the thioaliphatic SAMs.

In the following, we will give a brief description of the experimental procedure and setup. Thereafter, the results are presented and preliminarily discussed in section 3. An extended analysis of the data is given in section 4. Finally, the results are summarized in section 5.

## 2. Experimental Procedure

The substrates were prepared by evaporation of 100–300 nm of gold or silver on titanium-primed (5 nm) polished single-crystal Si(100) wafers (Silicon Sense). These polycrystalline films predominantly exhibit an (111) orientation as, e.g., concluded from the distinctive forward-scattering maxima in the angular distributions of the Au 4f and Ag 3d photoelectrons<sup>44</sup> and from the characteristic binding energy (BE) shift of the Au 4f surface component.<sup>45</sup> The BPT SAMs were formed by immersion of the substrates in an ethanolic 1mM solution of bis-(4'-methyl-1,1'-biphenyl-4-yl)-disulfide for 24 h. After the immersion, the samples were carefully rinsed and cleaned with ethanol and blown dry with pure nitrogen. The synthesis of bis-(4'-methyl-1,1'-biphenyl-4-yl)-disulfide is described elsewhere.<sup>46</sup>

Plasma treatment was performed in a special UHV preparation chamber attached to the analysis chamber (see ref 27 for details). The BPT/Au and BPT/Ag samples were simultaneously exposed to the afterglow plasma for 4 min. The samples were fixed on the sample holder in front of the outlet of a long quartz tube leading to the plasma glow discharge region. Plasma excitation in the glow-discharge region was performed by a microwave generator (~2.45 GHz, OPHOS Instruments Inc.) with a power of ~80 W. A flow rate of 500 cm<sup>3</sup>/min for N<sub>2</sub> gas (a purity of 99.9999%) was maintained by keeping a pressure of ~1 Torr in the plasma processing chamber. The pressure in the gas-discharged region was about 13 Torr.

The long pathway between the plasma glow discharge and afterglow region in the vicinity of the sample resulted in a low density and energy of the ionizing particles in the afterglow zone. As shown by the plasma characterization using a Langmuir probe, the density of electrons (and ions) in the downstream afterglow nitrogen microwave plasma and the electron temperature are  $1.37 \pm 0.22 \times 10^6$  particles/cm<sup>3</sup> and ~5500 K (~0.5 eV), respectively.<sup>27</sup> It can therefore be assumed that the major

impact of such a plasma treatment should be provided by long-living nitrogen and oxygen radicals such as N\*, N<sub>2</sub>\*, O\*, and O<sub>2</sub>\*.<sup>47–51</sup> The oxygen radicals originate from oxygen-containing species in the background gas and on the walls of the vacuum chamber. The relatively high pressure in the gas-discharged region and the plasma-processing chamber makes it very difficult to avoid these contaminations.<sup>27</sup>

In addition to the plasma treatment, we exposed the samples to 5 vol % diluted AAc monomers (using 95 vol % high purity N<sub>2</sub> as the carrier gas) to create the terminal O=C–OH group for the subsequent attachment of biologically relevant molecules. The exposure of AAc monomers to the plasma-treated SAMs was carried out either during the last minute of plasma processing or immediately after this processing was finished. Both exposure procedures led to similar results.

The characterization of the pristine, plasma-treated, and AAc-exposed BPT films was performed by high-resolution X-ray photoelectron spectroscopy (HRXPS) using synchrotron radiation and a CLAM-4 9-channeltron electron energy analyzer (VG Microtech). The measurements were carried out in an UHV analysis chamber attached to the U5 undulator beamline at the Synchrotron Radiation Research Center in Hsinchu, Taiwan. The samples were transferred from the preparation chamber directly to the analysis chamber. An excitation energy of 390 eV was utilized to measure the Au 4f, S 2p, and C 1s core level spectra, whereas the Ag 3d, N 1s, and O 1s spectra were acquired with a photon energy of 650 eV. The energy resolution was 0.25–0.3 eV. The energy scale was referenced to the pronounced Au 4f<sub>7/2</sub> peak of the BPT/Au sample at 84.00 eV.<sup>45</sup> The energy calibration was performed for every sample and after every change of the photon energy to exclude effects related to the instability of the monochromator. Special care was taken to avoid X-ray radiation-induced damage during spectra acquisition.<sup>7</sup>

The spectra were fitted using Voigt peak profiles and a Shirley background. To fit the S 2p<sub>3/2,1/2</sub> doublet, we used a pair of such peaks with the same fwhms, the standard<sup>52</sup> spin–orbit splitting of ~1.2 eV (verified by the fit), and the branching ratio of 2:1 (S 2p<sub>3/2</sub>/S 2p<sub>1/2</sub>). The resulting accuracy of the BE/fwhm values is ~0.05 eV.

## 3. Results

The HRXPS spectra of the pristine, plasma-treated, and AAc-exposed BPT SAMs are presented in panels a–c of Figures 1–6, respectively. The S 2p, C 1s, and O 1s spectra of BPT/Au are depicted in Figures 1, 3, and 5, and the corresponding spectra for BPT/Ag are given in Figures 2, 4, and 6, respectively. The normalization of the vertical scale is the same for all spectra for identical spectral regions. The differences in the signal-to-noise ratios in the C 1s and S 2p spectra for BPT/Au and BPT/Ag are related to different inelastic backgrounds provided by the inelastic electrons originated from the metal substrate. This background is comparably large in the case of Au, for which the most intense 4f doublet has a smaller BE (~84 eV) than the C1s and S2p peaks.

The spectra in Figures 1–6 are decomposed into the individual spectral components. The assignment of these components to the chemical moieties in the BPT films was performed according to refs 7, 10, 22, and 52–54. The normalized intensities of the C 1s and S 2p (only for BPT/Ag) peaks are indicated in Tables 1–3.

No traces of oxygen were found for the pristine films (see Figures 5a and 6a), which exclude contamination or partial oxidation of the film constituents or the substrate surface. The

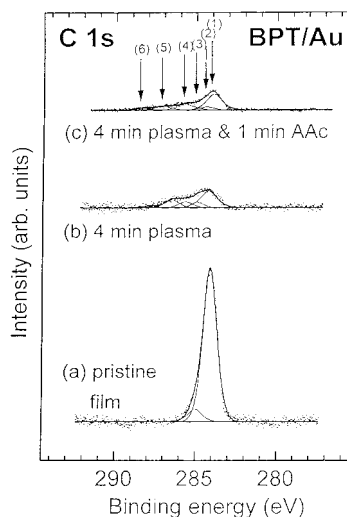


**Figure 1.** C 1s HRXPS spectra and peak assignments for the pristine (a), plasma-processed (b), and AAC-exposed (c) BPT/Au. Peak assignment: (1) 284.20 eV, aromatic chain; (2) 284.9 eV, shake-up satellite; (3) 285.6 eV, Ph\*-N; (4) 286.45 eV, Ph\*-O; (5) 287.9 eV, C=O; (6) 289.2 eV, O=C-OH.

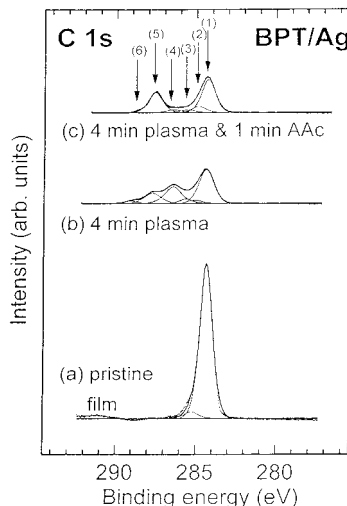


**Figure 2.** C 1s HRXPS spectra and peak assignments for the pristine (a), plasma-processed (b), and AAC-exposed (c) BPT/Ag. Peak assignment: (1) 284.20 eV, aromatic chain; (2) 284.9 eV, shake-up satellite; (3) 285.6 eV, Ph\*-N; (4) 286.45 eV, Ph\*-O; (5) 287.9 eV, C=O; (6) 289.2 eV, O=C-OH.

C 1s spectra of these films in Figures 1a and 2a exhibit an intense emission peak and a higher BE shoulder, related to aromatic carbon and a shake-up satellite, respectively.<sup>43,45,55</sup> The BE position of the main C 1s peak is  $\sim 284.2$  and  $\sim 284.3$  eV for BPT/Au and BPT/Ag, respectively, in good agreement with previous XPS<sup>43</sup> and HRXPS<sup>45,55</sup> results. The fwhm of this peak is 0.87–0.90 eV for both BPT/Au and BPT/Ag, which also correlates with earlier HRXPS data ( $\sim 0.77$  eV)<sup>45</sup> taken into account a better energy resolution of the experiments described in ref 45 ( $\sim 0.1$  eV).

The S 2p spectra of the pristine BPT films in Figures 3a and 4a exhibit a single S 2p doublet with BEs ( $S_{2p_{3/2}}$ ) of  $\sim 162.03$  and  $\sim 162.04$  eV for BPT/Au and BPT/Ag, respectively. The BE of the observed doublet is characteristic for the thiolate species bonded to noble metal surfaces<sup>7,42,45,56</sup> and agrees well with the analogous values of 162.08 ( $S_{2p_{3/2}}$  for BPT/Au) and 161.87 eV ( $S_{2p_{3/2}}$  for BPT/Ag) obtained in recent HRXPS study by Heister et al.<sup>45</sup> The fwhms of the  $S_{2p_{3/2}}$  and  $S_{2p_{1/2}}$  peaks are of special interest because of relatively large fwhm value

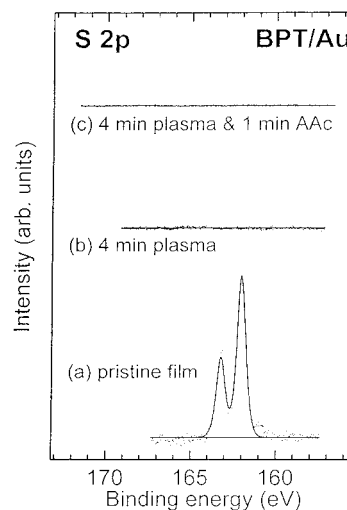


**Figure 3.** S 2p HRXPS spectra for the pristine (a), plasma-processed (b), and AAC-exposed (c) BPT/Au. The spectrum 3a reveals a single S 2p doublet (162.03 eV) related to the thiolate species bonded to noble metal surfaces.

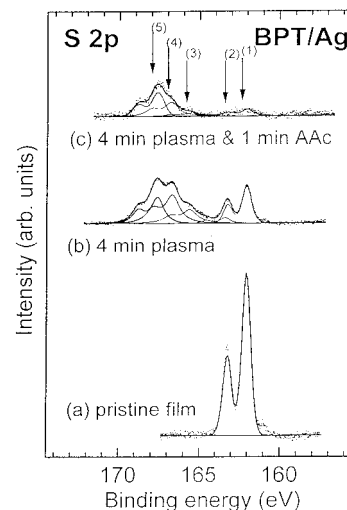


**Figure 4.** S 2p HRXPS spectra and peak assignments for the pristine (a), plasma-processed (b), and AAC-exposed (c) BPT/Ag. Peak assignment: (1) 162.04 eV, thiolate; (2) 163.4 eV, alkylsulfide; (3) 165.6 eV, SO; (4) 166.7 eV, SO<sub>2</sub>; (5) 167.6 eV, SO<sub>3</sub>.

for these peaks for BPT/Au in ref 45 as compared with those for BPT/Ag, AT/Au, and AT/Ag, which was presumably related to a poor quality of the BPT/Au film. The respective values are presented in Table 4 along with the S 2p fwhms of this study and those of ref 27. For both energy resolutions (0.25–0.3 eV for this study and ref 27, and  $\sim 0.1$  eV for ref 45), there is the same relation between the S 2p fwhms for BPT/Ag, AT/Au, and AT/Ag. At the same time, whereas the S 2p fwhm for BPT/Au in ref 45 is noticeably larger than the respective values for all other films, the S 2p fwhm for BPT/Au in this study is smaller as compared with the corresponding values for BPT/Ag, AT/Au, and AT/Ag measured at the same energy resolution. Applying the relation between the S 2p fwhms of BPT and AT films of this study and ref 27 to the respective values of ref 45, one gets a fwhm of  $\sim 0.50$  eV for BPT/Au, provided that the energy resolutions were the same as in ref 45. This value presumably corresponds to the fully commensurate arrangement of sulfur atoms on the (111) Au and Ag surfaces.<sup>45,55</sup> Such an arrangement obviously occurs in BPT/Au films of this study in full agreement with recent X-ray diffraction data,<sup>57</sup> whereas the

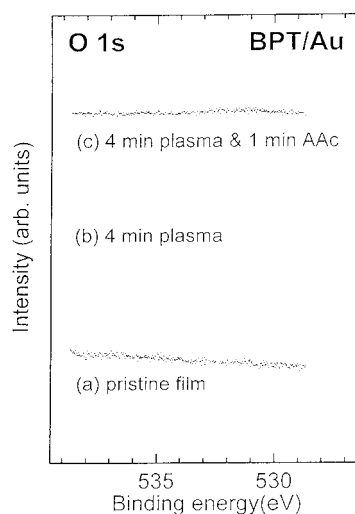


**Figure 5.** O 1s HRXPS spectra and peak assignments for the pristine (a), plasma-processed (b), and AAc-exposed (c) BPT/Au.

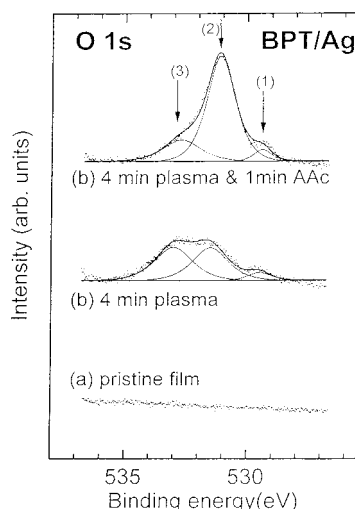


**Figure 6.** O 1s HRXPS spectra and peak assignments for the pristine (a), plasma-processed (b), and AAc-exposed (c) BPT/Ag. Peak assignment: (1) 529.5 eV, Ag<sub>2</sub>O; (2) 531.0 eV, C=O, O=C-OH, and SO<sub>n</sub>; (3) 533.0 eV, Ph-O\*.

**TABLE 1: Quantitative Evaluation of the C 1s Spectra for BPT/Au in Figure 1<sup>a</sup>**

	pristine	plasma exposure for 4 min	plasma exposure for 4 min and AAc exposure for 1 min
entire intensity	1 (100%)	0.25 (100%)	0.24 (100%)
benzene like + shake up	1 (100%)	0.15 (60%)	0.135 (55.8%)
benzene like-N		0.04 (16%)	0.014 (5.7%)
benzene like-O		0.05 (20%)	0.046 (19.6%)
C=O		0.01 (4%)	0.03 (12.3%)
O=C-OH			0.015 (6.6%)

<sup>a</sup> The peak intensities are normalized to the entire C 1s intensity for the pristine BPT/Au film (first value) and to the entire intensity of the respective C 1s spectrum (second value).

BPT/Au films of ref 45 are presumably noncommensurate. The quality of the BPT/Au films is assumed to depend strongly on the preparation condition: Both commensurate and noncommensurate arrangements of the BPT molecules on the (111) Au were observed for these systems and no reliable recipes, how to prepare a commensurately packed BPT SAM on Au(111), were so far developed.<sup>57</sup>

**TABLE 2: Quantitative Evaluation of the C 1s Spectra for BPT/Ag in Figure 2<sup>a</sup>**

	pristine	plasma exposure for 4 min	plasma exposure for 4 min and AAc exposure for 1 min
entire intensity	1 (100%)	0.53 (100%)	0.44 (100%)
benzene like + shake up	1 (100%)	0.26 (49%)	0.26 (59%)
benzene like-N		0.038 (6%)	0.02 (5%)
benzene like-O		0.13 (25%)	0.02 (5%)
C=O		0.085 (16%)	0.14 (31%)
O=C-OH		0.017 (4%)	

<sup>a</sup> The peak intensities are normalized to the entire C 1s intensity for the pristine BPT/Ag film (first value) and to the entire intensity of the respective C 1s spectrum (second value).

**TABLE 3: Quantitative Evaluation of the S 2p Spectra for BPT/Ag SAMs in Figure 4<sup>a</sup>**

	pristine	plasma exposure for 4 min	plasma exposure for 4 min and AAc exposure for 1 min
entire intensity	1 (100%)	0.89 (100%)	0.46 (100%)
thiolate	1 (100%)	0.21 (24%)	0.06 (14%)
alkylsulfide		0.04 (5%)	
sulfite		0.16 (18%)	0.04 (9%)
SO <sub>n</sub> (n = 1,2,3,...)		0.27 (30%)	0.16 (34%)
-(C <sub>6</sub> H <sub>4</sub> S)-		0.21 (23%)	0.20 (43%)

<sup>a</sup> The peak intensities are normalized to the entire S 2p intensity for the pristine BPT/Ag film (first value) and to the entire intensity of the respective S 2p spectrum (second value).

**TABLE 4: Comparison of the fwhms of the S 2p Peaks for the Thioaliphatic and Thioaromatic SAMs on Au and Ag Substrates<sup>a</sup>**

ref	energy resolution	AT/Au	AT/Ag	BPT/Au	BPT/Ag
45	0.1 eV	0.54 eV	0.58 eV	0.73 eV	0.53 eV
27	0.25–0.3 eV	0.67 eV	0.685 eV		
this study	0.25–0.3 eV			0.63 eV	0.655 eV

<sup>a</sup> Note that the data of this study and those of ref 27 were acquired under identical experimental conditions during the same beamtime.

The plasma treatment of the BPT SAMs results in noticeable changes in the C 1s and S 2p HRXPS spectra and in the appearance of the characteristic traces of oxygen and nitrogen in the O 1s and N 1s (not shown) spectra. The C 1s spectra for both BPT/Au and BPT/Ag change in a similar way as seen in Figures 1 and 2. The integral C 1s intensity and the intensity of the C 1s peak related to intact aromatic chains in the well-ordered BPT SAMs decrease (see also Tables 1 and 2), a downward shift and broadening of the latter peak occur, and a variety of new features on the higher BE side of the main emission evolve. The majority of these features could be assigned to different oxygen-containing moieties, and only the peak at ~285.6 eV is ascribed to a nitrogen-containing group. The occurrence of oxygen-containing species in the plasma-processed BPT/Ag is verified by the respective O 1s spectra in Figure 6b. The appearance of nitrogen-related species is supported by the N 1s spectra (not shown); the N 1s signal for the plasma-processed BPT/Ag is noticeably larger than that for BPT/Au, which suggests a higher percentage of nitrogen-derived species in the former film.

The observed changes are associated with the partial desorption of the BPT SAM as well as with decomposition and partial oxidation of the residual film resulting in its strong chemical



inhomogeneity.<sup>6,7,19,22</sup> The extent of these processes is noticeably larger in BPT/Au than in BPT/Ag. Moreover, the plasma-processed BPT/Au and BPT/Ag films are essentially different, as suggested by the respective S 2p spectra in Figures 3b and 4b. Whereas the S 2p doublet related to the pristine thiolate disappears completely after the plasma treatment of BPT/Au, this doublet is still observed in the S 2p spectrum for the plasma-treated BPT/Ag, even though with a considerably reduced intensity of 24% with respect to the pristine film (Figure 4b and Table 3). The disappearance of the pristine thiolate species in the plasma-processed BPT/Au is not accompanied by the appearance of new sulfur-derived species, the film does not contain any more sulfur. In contrast, pronounced emissions assigned to different sulfones (SO, SO<sub>2</sub>, and SO<sub>3</sub>)<sup>9,10</sup> evolve and become dominant in the S 2p spectrum for the plasma-processed BPT/Ag shown in Figure 4b. A comparably large intensity of these emissions can be related to different attenuation of the S 2p signals for the sulfone and thiolate species: Whereas the latter moieties are exclusively located at the SAM–substrate interface, the former species can be distributed over the whole film (similar to the irradiation-induced sulfur species).<sup>7</sup> Note that the above-mentioned partial desorption of the hydrocarbon layer affects also the intensity of the S 2p signal related to the thiolate species, which makes 24% the highest estimate for the amount of these species in the plasma-treated BPT/Ag.

Consideration of all XPS data implies a significant desorption of entire BPT moieties and a complete defragmentation of the residual hydrocarbon part for BPT/Au as a result of the plasma processing. The film loses its identity and becomes a mixture of saturated and nonsaturated hydrocarbons and their oxidative products. Alternatively, a part of intact BPT moieties are still retained after the plasma treatment in BPT/Ag, which is accompanied by a partial desorption of hydrocarbon fragments of the aromatic chains and a partial oxidation of the residual film. The plasma-induced desorption of sulfur-containing fragments from BPT/Ag occurs to a small extent, as implied by a relatively high S 2p intensity in Figure 4b.

Let us now consider the results of the AAc exposure. For BPT/Au, the attachment of AAc occurs to a very small extent. Only slight changes in the overall shape of the C 1s signal (Figure 1 parts b and c) and the N 1s spectral region are observed upon the AAc exposure. The respective intensity of the O 1s signal (Figure 5c) is also very small. Alternatively, AAc exposure provides a noticeable impact on the plasma-treated BPT/Ag films, as implied by comparison of the respective spectra in Figures 2, 4, and 6. The entire shape of the C 1s and O 1s signals changes: The intensities of the peaks related to the Ph–O and Ph–N (Ph = phenyl) species decrease noticeably, whereas the intensities of the C 1s and O 1s peaks assigned to the C=O and O=C–OH species increase by a factor of 2–3. In agreement with the C 1s spectra, there is also a reduction in the intensity of the N 1s feature at a BE of ~397 eV, related to Ph–N\*. In addition, there are essential changes in the S 2p spectra, in particular, a further reduction of the pristine thiolate species. All of these changes suggest a further damage of the BPT film and the attachment of a noticeable amount of AAc-derived species (C=O and O=C–OH) to the modified film.

#### 4. Discussion

The exposure of the BPT SAMs to the nitrogen–oxygen downstream microwave plasma results in an extensive damage and disordering of the initially well-ordered and chemically homogeneous monomolecular layers. The extent and character of these processes for BPT/Au are, however, noticeably different

from those for BPT/Ag. In the former system, desorption of the BPT moieties and defragmentation of the hydrocarbon residue occur to such a degree that the film loses completely its identity and becomes a mixture of saturated and nonsaturated hydrocarbons. In contrast, desorption of the entire BPT moieties occurs to a much smaller extent in BPT/Ag and only partial loss of hydrocarbon fragments and partial oxidation of the residual film takes place. A considerable part of intact BPT moieties (about 25%) in this film survives 4 min plasma treatment.

Plasma treatment generally involves bombardment of the substrate with ions, electrons, free radicals, and UV-light. The impact of every constituent depends on the plasma composition and the energy distribution, which is a function of the type and mode of plasma generation. In our study, the energy of the electrons and ions in the downstream microwave plasma (~0.5 eV)<sup>27</sup> is noticeably lower than the threshold for the electron-induced damage in AT SAMs (~5–7 eV).<sup>17,21</sup> This suggests that the processes associated with electron irradiation, such as cleavage of C–H bonds and subsequent cross-linking between the adjacent aromatic chains do not occur to a significant extent in the present case. In fact, we do not observe that the orientational order and anchoring to the substrate are still retained upon the plasma treatment as it occurs in the case of electron irradiation of the thioaromatic SAMs (because of the above-mentioned cross-linking).<sup>23,39,40</sup> It is also not expected that low-energy ions affect the BPT films to a noticeable extent. Although the ion-induced damage in thioaromatic films was not investigated yet, the analogous process in AT SAMs<sup>3</sup> has no resemblance with the plasma-induced changes observed in this study.

We believe that the major impact of the nitrogen–oxygen downstream microwave plasma treatment on BPT SAMs on Au and Ag is provided by long-living nitrogen and oxygen radicals such as N\*, N<sub>2</sub>\*, O\*, and O<sub>2</sub>\* and oxygen-containing reactive species, as observed for thioaliphatic SAMs.<sup>27</sup> The changes caused by the plasma treatment in the BPT films resemble the changes occurring in AT SAMs at UV exposure in the presence of air.<sup>8–12</sup> Considering that the latter changes are predominately caused by oxygen-derived reactive species generated by the UV light, a dominant role of atomic oxygen and oxygen radicals can also be assumed in the present case. Note that in addition to the photooxidation of the S–substrate interface and partial desorption of the hydrocarbon fragments typical for the UV-exposure, we observe the complete damage of the S–substrate interface in BPT/Au and partial oxidation of the hydrocarbon residue in BPT/Ag and BPT/Au.<sup>9,10,12</sup> These processes can be at least partly related to the effects mediated by a small fraction of “hot” ionizing particles (electrons and ions), which are still present in a low-energy plasma. These particles can promote the oxidation of the alkyl matrix and a larger damage at the S–Au interface.

On the basis of the results of the UV photooxidation studies of AT SAMs<sup>9</sup> and the S 2p spectra of this article, we assume that the exposure of BPT SAMs to the afterglow nitrogen–oxygen plasma results in the penetration of oxygen radicals to the film–substrate interface and the subsequent oxidation of the thiolate species, which can further lead to a complete cleavage of the substrate–S bond. The penetration of oxygen radicals can only occur through defective sites in the initially densely packed films and should be characterized by comparable rates in both systems considering only a slightly higher packing density of BPT/Ag<sup>43</sup> and assuming a similar defect density in BPT/Au and BPT/Ag. It should be the anchoring to the substrate

or, in other words, the strength of the thiolate–substrate bond that is of major importance for the efficiency of the oxidation and desorption processes at the S–substrate interface. In the case of Au, all thiolate–Au bonds are cleaved during 4 min of plasma processing with the subsequent desorption of BPT molecules. In the case of Ag, only part of the pristine thiolate–Ag bonds are destroyed, and the evolving sulfone species get trapped at the film–substrate interface and in the aromatic matrix. This difference suggests a stronger thiolate–substrate bond in the thioaromatic films on Ag as compared to Au. Considering that the analogous difference is also assumed for the thioaliphatic SAMs,<sup>3,11,22,41</sup> one can regard it as a general property of thiol-derived SAMs. Even if the character of long-chain spacer and the identity of tail group affect the strength of the thiolate–metal bond to some extent, the major impact is obviously provided by the identity of the substrate.

This assumption helps to explain the observed differences in the reaction of thioaromatic and thioaliphatic SAMs toward electron irradiation and plasma treatment. In the case of electron irradiation of the thioaromatic SAMs, cross-linking processes in the aromatic matrix are of major importance; the respective quasipolymerization stabilizes the film and hinders any molecular or atomic shift or movement at and in the vicinity of the thiolate–substrate interface.<sup>23</sup> Alternatively, the cross-linking processes evolve comparatively slowly in the thioaliphatic SAMs. Conformational changes and atomic shifts are therefore less hindered, and the SAMs become heavily damaged as a result of electron irradiation. The damage of the aliphatic matrix is practically unaffected by the strength of the thiolate–substrate bond and is essentially similar for AT/Au and AT/Ag.<sup>22</sup>

In the case of free radical-dominant plasma treatment (and, presumably, in the case of UV photooxidation), not the character of the long chain spacer but the strength of the thiolate–substrate bond and the defect density are of significance. Both thioaliphatic<sup>27</sup> and thioaromatic films become damaged in a similar way, with the damage of the latter SAMs being even more extended. At the same time, both thioaliphatic<sup>27</sup> and thioaromatic films on Ag substrates are much more stable with respect to the plasma treatment than the same films on Au substrates.

The larger damage of the thioaromatic films in this study as compared to the octadecanethiol [C18: CH<sub>3</sub>–(CH<sub>2</sub>)<sub>17</sub>–SH] SAMs in ref 27 can be explained by two reasons considering that the primary process is the defect-mediated penetration of the oxygen radicals to the S–substrate interface. First, the C18 molecules are longer than the BPT species: a stronger intermolecular interaction and a better ordering can then be expected for the C18 SAMs. Second, the defect density in thioaromatic and thioaliphatic SAMs can be principally different (the relation of the defect densities is not known by present). The characterization of the plasma-induced changes in the thioaromatic and thioaliphatic SAMs of the same thickness can help to clarify the latter issue.

Let us now turn to the AAc exposure. Contrary to the initial intention, not softly processed but completely (BPT/Au) or strongly (BPT/Ag) damaged BPT films were exposed to AAc monomer. A noticeable AAc attachment occurred only to BPT/Ag. We believe that AAc reacted with radicals and chemically active defective sites of the latter film. Hydrocarbon residues and adsorbate-free parts of the metal surface, which can appear after a complete removal of sulfur in BPT/Au, did not react with the AAc species. Plasma treatment of a shorter duration or exposure to the less reactive nitrogen plasma can probably

provide better prerequisites for the AAc attachment than it has been achieved in our experiments.

## 5. Summary

Synchrotron-based high-resolution photoelectron spectroscopy was applied to study the modification of the thioaromatic BPT SAMs on gold and silver substrates by nitrogen–oxygen downstream microwave plasma and the attachment of the AAc monomer to the plasma-modified films. It was found that the plasma treatment did not result in a “soft” modification of the BPT films but in their massive damage and disordering, with the extent and character being noticeably different for BPT/Au and BPT/Ag. In the former film, a profound desorption and defragmentation of the BPT moieties occurred. No original thiolate species or even sulfur-containing species could be found after 4 min plasma exposure. The film lost completely its identity and became a mixture of saturated and nonsaturated hydrocarbons and their oxidative products. At the same time, only partial desorption of hydrocarbon fragments and partial oxidation of the residual film took place for BPT/Ag, in which a noticeable part of intact BPT moieties survived the plasma treatment.

The differences in the response of BPT/Au and BPT/Ag toward the plasma treatment are assumed to be predominantly related to the different strengths of the thiolate–substrate bond in these two systems. Considering that the analogous difference was also postulated for the thioaliphatic SAMs,<sup>3,11,22,27,41</sup> one can regard it as a general property of thiol-derived SAMs.

The extent of the AAc attachment to the plasma-treated BPT/Ag was much larger than that to the hydrocarbon residues in the case of BPT/Au. The attachment of the AAc monomers to BPT/Ag occurred presumably through their reaction with radicals and chemically active defective sites.

Some other interesting findings should be mentioned. First, the comparison of the S 2p spectra of this study with the analogous spectra of BPT and AT SAMs acquired at the comparable<sup>27</sup> and better<sup>45,55</sup> energy resolution implies that the natural width of the S 2p peaks for BPT/Au is ~0.50 eV, which is the smallest value observed for the thiol-derived SAMs.<sup>45,55</sup> This suggests a commensurate arrangement of the thiolate headgroups in the BPT SAMs on the (111) Au surface in full agreement with previous X-ray diffraction results.<sup>57</sup> Second, considering that the major impact of the plasma exposure in the present case is presumably provided by long-living oxygen radicals and oxygen-containing reactive species, an oxygen contamination has to be avoided if one intends to perform a “soft” modification of a thin organic film by a plasma treatment.

**Acknowledgment.** We thank Haitao Rong (Universität Heidelberg) and Manfred Buck (University of St Andrew) for providing us with the BPT substance, Karin Heister (Universität Heidelberg) and Y.-Te Wu (CYCU) for help in the sample preparation and data processing, and Prof. T. -J. Chuang (National Taiwan University) for providing experimental equipment at the U5 end station and two studentships under the Taiwan Ministry of Education Grant No. 90-N-FA01-2-4-5. This work has been supported by the National Science Council of Taiwan under Grant Nos. 90-2320-B-033-005-Y, 89-2112-M-213-016, and 90-2112-M-213-003, by the German Bundesministerium für Bildung und Forschung under Grant Nos. 05 S.F.8VHA 1 and GRE1HD, and by the DAAD-NSC exchange program under the PPP Grant No. 10.

## References and Notes

- (1) Ulman, A. *An Introduction to Ultrathin Organic Films: Langmuir–Blodgett to Self-Assembly*; Academic Press: New York, 1991. Ulman, A. *Chem. Rev.* **1996**, *96*, 1533.
- (2) Ulman, A., Ed.; *Thin films: self-assembled monolayers of thiols*, Academic Press: San Diego, CA, 1998.
- (3) Chenakin, S. P.; Heinz, B.; Morgner, H. *Surf. Sci.* **1999**, *421*, 337.
- (4) Laibinis, P. E.; Graham, R. L.; Biebuyck, H. A.; Whitesides, G. M. *Science* **1991**, *254*, 981.
- (5) Jäger, B.; Schürmann, H.; Müller, H. U.; Himmel, H. J.; Neumann, M.; Grunze, M.; Wöll, Ch. *Z. Phys. Chem.* **1997**, *202*, 263.
- (6) Wirde, M.; Gelius, U.; Dunbar, T.; Allara, D. L. *Nucl. Instrum. Methods Phys. Res. B* **1997**, *131*, 245.
- (7) Heister, K.; Zharnikov, M.; Grunze, M.; Johansson, L. S. O.; Ulman, A. *Langmuir* **2001**, *17*, 8.
- (8) Lewis, M.; Tarlov, M. J.; Carron, K. *J. Am. Chem. Soc.* **1995**, *117*, 9574.
- (9) Hutt, D. A.; Leggett, G. J. *J. Phys. Chem. B* **1996**, *100*, 6657.
- (10) Hutt, D. A.; Cooper, E.; Leggett, G. J. *J. Phys. Chem. B* **1998**, *102*, 174.
- (11) Cooper, E.; Leggett, G. J. *Langmuir* **1998**, *14*, 4795.
- (12) Riely, H.; Kendall, G. K.; Zemicael, F. W.; Smith, T. L.; Yang, S. *Langmuir* **1998**, *14*, 5147.
- (13) Baer, D. R.; Engelhard, M. H.; Schulte, D. W.; Guenther, D. E.; Wang, L.-Q.; Rieke, P. C. *J. Vac. Sci. Technol. A* **1994**, *12*, 2478.
- (14) Rowntree, P.; Dugal, P. C.; Hunting, D.; Sanche, L. *J. Phys. Chem.* **1996**, *100*, 4546.
- (15) Seshadri, K.; Froyd, K.; Parikh, A. N.; Allara, D. L.; Lercel, M. J.; Craighead, H. G. *J. Phys. Chem.* **1996**, *100*, 15900.
- (16) Müller, H. U.; Zharnikov, M.; Völkel, B.; Schertel, A.; Harder, P.; Grunze, M. *J. Phys. Chem. B* **1998**, *102*, 7949.
- (17) Olsen, C.; Rowntree, P. A. *J. Chem. Phys.* **1998**, *108*, 3750.
- (18) Zerulla, D.; Chasse, T. *Langmuir* **1999**, *15*, 5285.
- (19) Zharnikov, M.; Frey, S.; Götzhäuser, A.; Geyer, A.; Grunze, M. *Phys. Chem. Phys.* **1999**, *1*, 3163.
- (20) Heister, K.; Frey, S.; Götzhäuser, A.; Ulman, A.; Zharnikov, M. *J. Phys. Chem. B* **1999**, *103*, 11098.
- (21) Huels, M. A.; Dugal, P. C.; Sanche, L. To be published.
- (22) Zharnikov, M.; Frey, S.; Heister, K.; Grunze, M. *Langmuir* **2000**, *16*, 2697.
- (23) Frey, S.; Rong, H.-T.; Heister, K.; Yang, Y.-J.; Buck, M.; Zharnikov, M. *Langmuir* **2002**, *18*, in press.
- (24) Maoz, R.; Cohen, S. R.; Sagiv, J. *Adv. Mater.* **1999**, *11*, 55.
- (25) Lercel, M. J.; Craighead, H. G.; Parikh, A. N.; Seshadri, K.; Allara, D. L. *J. Vac. Sci. Technol. A* **1996**, *14*, 1844.
- (26) Unger, W. E. S.; Lippitz, A.; Gross, Th.; Friedrich, J. F.; Wöll, Ch.; Nick, L. *Langmuir* **1999**, *15*, 1161.
- (27) Liao, J.-D.; Wang, M.-C.; Weng, C.-C.; Klauser, R.; Frey, S.; Zharnikov, M.; Grunze, M. *J. Phys. Chem. B* **2002**, *106*, 77.
- (28) Tiberio, R. C.; Craighead, H. G.; Lercel, M. J.; Lau, T.; Sheen, C. W.; Allara, D. L. *Appl. Phys. Lett.* **1993**, *62*, 476.
- (29) Lercel, M. J.; Tiberio, R. C.; Chapman, P. F.; Craighead, H. G.; Sheen, C. W.; Parikh, A. N.; Allara, D. L. *J. Vac. Sci. Technol. B* **1993**, *11*, 2823.
- (30) Lercel, M. J.; Redinbo, G. F.; Pardo, F. D.; Rooks, M.; Tiberio, R. C.; Simpson, P.; Craighead, H. G.; Sheen, C. W.; Parikh, A. N.; Allara, D. L. *J. Vac. Sci. Technol. B* **1994**, *12*, 3663.
- (31) Lercel, M. J.; Redinbo, G. F.; Rooks, M.; Tiberio, R. C.; Craighead, H. G.; Sheen, C. W.; Allara, D. L. *Microelectron. Eng.* **1995**, *27*, 43.
- (32) Lercel, M. J.; Rooks, M.; Tiberio, R. C.; Craighead, H. G.; Sheen, C. W.; Parikh, A. N.; Allara, D. L. *J. Vac. Sci. Technol. B* **1995**, *13*, 1139.
- (33) Müller, H. U.; David, C.; Völkel, B.; Grunze, M. *J. Vac. Sci. Technol. B* **1995**, *13*, 2846.
- (34) David, C.; Müller, H. U.; Völkel, B.; Grunze, M. *Microelectron. Eng.* **1996**, *30*, 57.
- (35) Hild, R.; David, C.; Müller, H. U.; Völkel, B.; Kayser, D. R.; Grunze, M. *Langmuir* **1998**, *14*, 342.
- (36) Sugimura, H.; Ushiyama, K.; Hozumi, A.; Takai, O. *Langmuir* **2000**, *16*, 885.
- (37) Götzhäuser, A.; Geyer, W.; Stadler, V.; Eck, W.; Grunze, M.; Edinger, K.; Weimann, Th.; Hinze, P. *J. Vac. Sci. Technol. B* **2000**, *18*, 3414.
- (38) Götzhäuser, A.; Eck, W.; Geyer, W.; Stadler, V.; Weimann, T.; Hinze, P.; Grunze, M. *Adv. Mater.* **2001**, *13*, 806.
- (39) Geyer, W.; Stadler, V.; Eck, W.; Zharnikov, M.; Götzhäuser, A.; Grunze, M. *Appl. Phys. Lett.* **1999**, *75*, 2401.
- (40) Eck, W.; Stadler, V.; Geyer, W.; Zharnikov, M.; Götzhäuser, A.; Grunze, M. *Adv. Mater.* **2000**, *12*, 805.
- (41) Jaffey, D. M.; Madix, R. J. *Surf. Sci.* **1994**, *311*, 159.
- (42) Laibinis, P. E.; Whitesides, G. M.; Allara, D. L.; Tao, Y.-T.; Parikh, A. N.; Nuzzo, R. G.; *J. Am. Chem. Soc.* **1991**, *113*, 7152.
- (43) Frey, S.; Stadler, V.; Heister, K.; Zharnikov, M.; Grunze, M.; Zeysing, B.; Terfort, A. *Langmuir* **2001**, *17*, 2408.
- (44) Köhn, F. Ph.D. Thesis, Universität Heidelberg, Heidelberg, Germany, 1998.
- (45) Heister, K.; Zharnikov, M.; Grunze, M.; Johansson, L. S. O. *J. Phys. Chem. B* **2001**, *105*, 4058.
- (46) Rong, H.-T. Ph.D. Thesis, Universität Heidelberg, Heidelberg, Germany, 2001.
- (47) Grill, A. *Cold Plasma in Materials Fabrication: from fundamentals to applications*; IEEE Press: Piscataway, NJ, 1993; p 129–137.
- (48) Wolf, B. H., Ed. *Handbook of Ion Sources*; CRC Press: Boca Raton, FL, 1995; Chapter 2.
- (49) Spanel, P. *Int. J. Mass Specrom. Ion Processes* **1995**, *149–150*, 299.
- (50) Chen, Y.-W.; Liao, J.-D.; Kau, J.-Y.; Huang, J.; Chang, W.-T.; Chen, C.-W. *Macromolecules* **2000**, *33*, 5638.
- (51) Tyan, Y.-C.; Liao, J.-D.; Klauser, R.; Wu I.-D.; Weng, C.-C. *Biomaterials* **2002**, *23*, 67.
- (52) Moulder, J. F.; Stickle, W. E.; Sobol, P. E.; Bomben, K. D. *Handbook of X-ray Photoelectron Spectroscopy*, Perkin-Elmer Corporation: Eden Prairie, MN, 1992.
- (53) Siegbahn, K.; Nordling, C.; Fahlman, A.; Nordberg, R.; Hamrin, K.; Hedman, J.; Johansson, G.; Bergmark, T.; Karlsson, S.-E.; Lindgren, I.; Lindberg, B. *Nova Acta Regiae Soc. Sci. Ups.* **1967**, *IV*, 118.
- (54) Lee, M.-T.; Hsueh, C.-C.; Freund, M. S.; Ferguson, G. S. *Langmuir* **1998**, *14*, 6419.
- (55) Heister, K.; Rong, H.; Buck, M.; Zharnikov, M.; Grunze, M.; Johansson, L. S. O. *J. Phys. Chem. B* **2001**, *105*, 6888.
- (56) Himmelhaus, M.; Gauss, I.; Buck, M.; Eisert, F.; Wöll, Ch.; Grunze, M. *J. Electron Spectrosc. Relat. Phenom.* **1998**, *92*, 139.
- (57) Leung, T. Y. B.; Schwartz, P.; Scoles, G.; Schreiber, F.; Ulman, A. *Surf. Sci.* **2000**, *458*, 34.